Regularity and synchrony in motor proteins

R. E. Lee DeVille and Eric Vanden-Eijnden

Courant Institute of Mathematical Sciences, New York University, New York, NY 10012

Corresponding author:

R. E. Lee DeVille

Courant Institute of Mathematical Sciences

251 Mercer St.

New York, NY 10012

deville@cims.nyu.edu

FAX: +1 212-995-4121

Regularity and synchrony in motor proteins

R. E. Lee DeVille and Eric Vanden-Eijnden*

October 24, 2006

Abstract

We investigate the origin of the regularity and synchrony which have been observed in numerical experiments of two realistic models of molecular motors, namely Kolomeisky-Fisher's model of myosin V for vesicle transport in cells and Duke's model of myosin II for sarcomere shortening in muscle contraction. We show that there is a generic organizing principle behind the emergence of regular gait for a motor pulling a large cargo and synchrony of action of many motors pulling a single cargo. These results are surprising in that the models used are inherently stochastic, and yet they display deterministic behaviors in the parameter range relevant for the experiments. Our results also show that these behaviors are not tied to the particular models used in these experiments, but rather are generic to a wide class of molecular motor models.

1 Introduction

Motor proteins are tiny nanometer-sized engines capable of generating motion at the microscopic level (for reviews see e.g. [1, 24]). Many different types of motor proteins exist in eucaryotic cells in which they move various organelles and vesicles from one place to another. Other types of motor proteins are also responsible for sarcomere shortening in muscle contraction and cell division. Typically, motor proteins bind to filament tracks made of actin or microtubules and move along them using the energy generated by a chemical reaction known as hydrolysis during which a molecule of adenosine triphosphate (ATP) is converted into a molecule of adenosine diphosphate (ADP) and a phosphate. The part of the motor protein which binds to the track is called the "motor head", and this is the part of the motor which hydrolyzes ATP – attached to this head via some tether is the actual cargo that the motor carries. The hydrolysis process is part of a complicated cycle during which the motor protein experiences conformational changes together with binding and unbinding to the track, the net effect of which is the motion by one step along the track (typically one step is a few nanometers long).

Motor proteins come in a variety of forms (including, amongst many others, the myosin superfamily and the kinesin family [1, 24]) and have a wide variety of motile properties. For example, the kinesin and the myosin V motor proteins are known to be highly processive, and can undergo hundreds of cycles without disassociating from its track. On the other hand, myosin II motor protein in skeletal muscle disassociates itself between every cycle. While ATP hydrolysis is the main source of energy of motor proteins, the thermal perturbations created by the surrounding solvent also play an essential role [2]. Indeed, it is the solvent which drives the conformational changes of the molecule responsible for the binding and hydrolysis of ATP [19]. The solvent also helps in the binding-unbinding cycle which propels the motor by one step along its track. Thus, unlike macroscopic motors, the presence of random perturbations is crucial for the operation of motor proteins.

A wide variety of models have been proposed for motor proteins and, consistent with the observation that the motors operate in the thermal bath of the solvent, these models usually have a stochastic component. They include Brownian ratchets [18], continuous-time Markov chain models on discrete state-space, and

*Courant Institute of Mathematical Sciences, New York University, New York, NY 10012

cross-bridge models [10]. In this paper, we will focus on two such models, though the conclusions that we draw from them will be shown to be applicable to a much wider class. The first is a model (or rather a class of models) due to Kolomeisky and Fisher [11, 12, 16], which was primarily designed for myosin-V, although it has also been successfully applied to other motor proteins such as kinesin. In this model, the motor can only sit at a discrete set of sites along its track, and steps forward or backward as a Markov jump process. The rates of the jumps depend on the force applied by the cargo, which in turns depends on the distance between the cargo and the motor. Kolomeisky-Fisher's model can predict many quantities of the motor dynamics, e.g. the mean and variance of its velocity, its stall force, etc. As mentioned earlier, this model has been applied to myosin-V [16] and kinesin [12], where it has been very successful in matching certain types of experimental data. In [21], a series of numerical experiments have been conducted using Kolomeisky-Fisher's model in situations where the protein motor carries a heavy cargo and it was observed that the presence of this cargo regularizes dramatically the gait of the motor. One purpose of the present paper is to explain mathematically the mechanism behind the emergence of this regularity and show that it is, in fact, generic: the gait of motors modeled by continuous-time Markov chain models or Brownian ratchets will become regular when they carry a heavy cargo. As explained below, this is an instance of self-induced stochastic resonance in the context of Markov chains.

The second model which we will investigate in some detail in a model proposed by Duke [7] for the description of myosin II in the context of sarcomere shortening in muscle contraction. It is known that the mechanism of muscle contraction is due to the relative sliding of a large myosin II molecule with an actin filament, and the work which carries out this sliding is done by many myosin heads. The myosin heads can detach from and reattach to the actin filament, but they can also "extend" while attached and apply a larger force to the actin filament – this is the well-known "lever-arm" model. In Duke's paper [7], these events (extending, detaching, reattaching of each of the myosin heads) are modeled as force-dependent Markov jump processes whose rates are matched with the data from mechanochemical studies. The remarkable property observed by Duke in his model is the ability of the population of motors to act in synchrony, or near-synchrony, under certain applied forces. More specifically, it is observed that the system repeatedly finds itself in a state where almost all of the heads are attached, and then a vast majority of the heads extend at almost the same time, so that the dynamics of the sarcomere shortening are nearly stepwise motion when sufficient force is applied. Here, we explain this phenomenon mathematically and show that it is very generic: a large population of motor proteins pulling a single load tends to act in synchrony.

To make these points, we will first analyze a simpler model with three adjustable parameters, which can be thought of as crude caricature of Kolomeisky-Fisher's and Duke's but retains the main features leading to regularity and synchrony. The simple model is studied in section 2 where we show rigorously that, in specific scaling limits, it displays either regularity (section 2.3) or synchrony (section 2.4). In section 3 we then come back to Kolomeisky-Fisher's and Duke's models. In section 3.1 we show that the phenomenon analyzed in the simple model also explains the regularity observed in numerical experiments with myosin V. In section 3.2 we tie the mechanism behind the synchrony of action of myosin II in muscle contraction to the one we observed in the simple model. Finally, in Section 4, we discuss the genericity of our results and speculate briefly about their biological implications.

2 Regularity and synchronization in a simple illustrative model

In this section we analyze a simple model of a population of molecular motors pulling a common cargo (see figure 1 for a schematic representation). While simple, this model retains the main features of the more realistic models that we will consider in section 3. In particular, the motors are modeled by a Markov jump process with forward rates which depend on the force applied by the cargo. When any motor jumps, it moves forward one step (for simplicity, we prohibit the possibility of a motor stepping backwards). A forward motion by a motor causes the force on the cargo to increase to the right, and the force on the motor which jumped to increase to the left. This decreases the rate of activation of this motor, making it less likely to jump. The motion of the cargo, on the other hand, is modeled by a simple ordinary differential equation in which the cargo velocity is proportional to the force applied on it by the motors with a proportionality

constant inversely proportional to the mass of the cargo (overdamped limit).

We consider this model in two special scaling limits. In the first, we fix the size of the population and then take the noise amplitude to be very small and the mass of the cargo be very large. We show that in this scaling limit, the motion becomes regular: all the motors jump at the same time, and the time between these collections of jumps is constant. In the second scaling limit we take the friction on the cargo to be not too large, but take the amplitude of the noise to be small and the number of motors to be very large. In this limit we also see a synchronization of the motors: they all jump together and the time between jumps is constant as well.

Although we observe similar regularity and synchrony in these two limits, we stress that these behaviors arise from completely different causes. In the first case, regularity is a manifestation of self-induced stochastic resonance [14, 15, 17, 5, 4]. In particular, it is the slow relaxation of the cargo which makes the system predictable. Moreover, the system is always in an unstable state and the cargo never reaches equilibrium. In the second case, regularity comes from a sort of auto-catalysis effect: the forward step by any motor allows the other motors to jump more easily. This leads to a cascade phenomenon where, after a regular period of time during which a few motors jump one step forward, all the remaining ones suddenly jump one step forward. The process then repeats itself indefinitely. In this limit, from the point of view of the motors, the relaxation timescale of the cargo becomes essentially zero and the cargo is essentially always at force equilibrium, unlike what happens in the first scaling limit.

In Section 3 below, we show that these models are similar to realistic models used in the biological literature. We show in Section 3.1 how the first scaling limit corresponds to the dynamics of a processive molecular motor, or a small population of processive molecular motors, of Kolomeisky-Fisher type. In Section 3.2 we show that the second scaling limit explains aspects of the dynamics of large populations of nonprocessive motors modeled by the cross-bridge model of Duke [7] for muscle contraction.

2.1 Intuitive description of the process

Our simple model consists of $K \geq 1$ motors pulling a single cargo (see Fig. 1 for a schematic representation). The motors are modeled as point particles moving on a track whose positions are specified by $x_k \in \mathbb{Z}$, $k = 1, \ldots, K$. The cargo is also represented as a point particle whose position is specified by $y \in \mathbb{R}$. Thus, the motors move discretely along the track and take steps of size 1. In contrast, the cargo moves continuously.

Each motor is tethered to the cargo in the same way and exerts a force on this cargo which depends only on the distance between the cargo and the motor. Thus, the total force on the cargo is assumed to be of the form

$$F(\boldsymbol{x}, y) = \sum_{k=1}^{K} f(x_k - y).$$

where $f(\cdot)$ is some monotone increasing function such that $f(0) = 0$. Consistent with the viscous effect being very important at the scale at which this system operates, we assume that the dynamics of the cargo is overdamped, i.e. it is governed by

$$\frac{dy}{dt} = \gamma^{-1} F(\boldsymbol{x}, y). \tag{1}$$

where γ is the friction coefficient (with dimension of a mass divided by a time).

Turning now to the dynamics of the motors, we assume that each can only move forward by unit steps and do so as a Markov jump process. The rates of jump are taken to mimic the escape from the potential well consistent with the force on the motor applied by the cargo. Suppose that the distance between the kth motor and the cargo is $x_k - y$ so that the force exerted by the cargo on the motor is $-f(x_k - y)$. In order to jump forward by one step on the track, the motor must overcome the potential barrier

$$\Delta V(x_k - y) = V(x_k - y + 1) - V(x_k - y),$$

where

$$V(z) = \int_0^z f(\zeta)\, d\zeta.$$

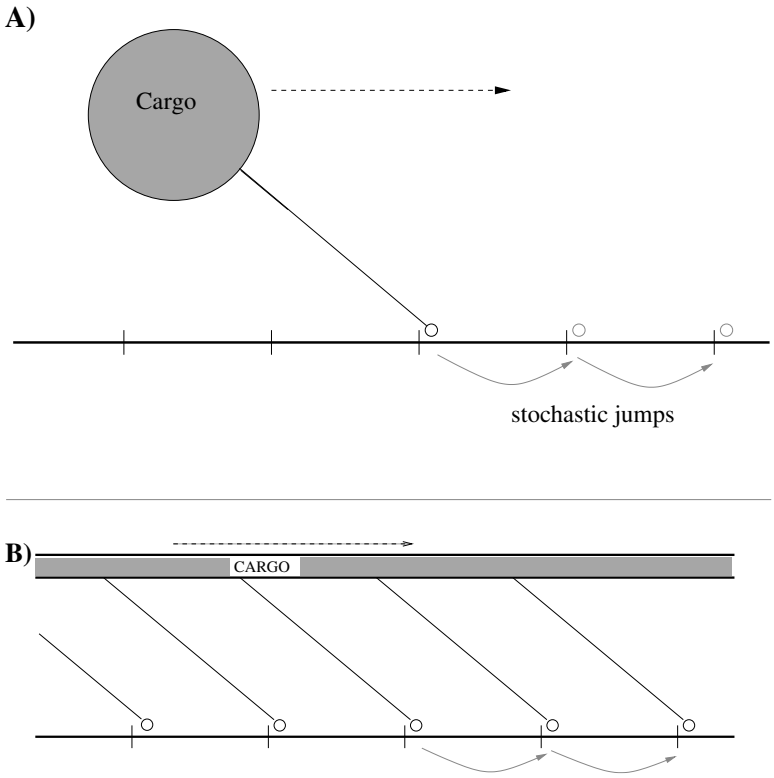

Figure 1: Two schematics of the motor population coupled to a common cargo. The motors jump stochastically between the different sites along the track, and the cargo moves continuously under the applied force. In panel A, we represent one motors carrying a cargo to the right; this can be thought of as a schematic for a motor protein transporting a cargo in a cell. In panel B, we show an equivalent formulation of many motors coupled to a common cargo. Here we have drawn things so that the cargo is not localized at a point, but is extended, bringing to mind muscle contraction models.

Consistent with the jump being modeled as an escape out of this well, we assume that in any sufficiently small time Δt, the motor jumps one step forward with probability given by $\lambda(x_k - y)\Delta t$ where

$$\lambda(x_k - y) = \exp(-\epsilon^{-1}\Delta V(x_k - y)). \tag{2}$$

Here $\epsilon > 0$ is a parameter with the dimension of an energy which may be thought of as the temperature of the system.

Equation (1), together with the the rule above for the motion of the motors, specifies completely the dynamics of our model, as shown in section 2.2. This model has three parameters: K, γ and ϵ, and below, we will analyze the dynamics as these parameters are varied in two specific ways in sections 2.3 and 2.4.

2.2 Precise definition of the process

Here we give a precise definition of the stochastic process which couples the discrete jumps of the motors to the continuous motion of the cargo. This process is slightly nonstandard because the rates at which the motors jump forward are not fixed but vary as the cargo moves. From the rule above, given $\boldsymbol{x} = (x_1, \ldots, x_K)$ and y and a sufficiently small time Δt, the probability of a motor stepping forward is $\Lambda(\boldsymbol{x}, y)\Delta t$, where $\Lambda(\boldsymbol{x}, y)$

is the total intensity to jump forward,

$$\Lambda(\boldsymbol{x}, y) = \sum_{k=1}^{K} \lambda(x_k - y),$$

and the probability of it being the kth motor is

$$p_k(\boldsymbol{x}, y) := \frac{\lambda(x_k - y)}{\Lambda(\boldsymbol{x}, y)}. \tag{3}$$

Now, define the map $\varphi_{\boldsymbol{x},t}(A)$ as the solution at time t of (1) with initial condition $y(0) = A$ and $\boldsymbol{x}$ fixed and let $\tau(\boldsymbol{x}, A)$ be the random variable with cumulative probability distribution

$$\mathbb{P}\{\tau(\boldsymbol{x}, A) \leq t\} = 1 - \exp\left(-\int_0^t \Lambda(\boldsymbol{x}, \varphi_{\boldsymbol{x},t'}(A))\, dt'\right). \tag{4}$$

Then, given an initial condition $(X(0), Y(0))$, the process $(X(t), Y(t))$, where $X\colon \mathbb{R} \to \mathbb{Z}^K, Y\colon \mathbb{R} \to \mathbb{R}$, can be defined as follows. Set $\tau_0 = 0$ and for $n \geq 1$, let τ_{n+1} be a sample of

$$\tau(X(\tau_n), Y(\tau_n)).$$

Define

$$Y(t) = \varphi_{X(\tau_n),t-\tau_n}(Y(\tau_n)), \quad t \in [\tau_n, \tau_{n+1}],$$

and say that $X(t)$ is constant on $[\tau_n, \tau_{n+1})$. Define σ_{n+1} by

$$\mathbb{P}(\sigma_{n+1} = k) = p_k(X(\tau_{n+1}), Y(\tau_{n+1})).$$

Finally, define

$$X_k(\tau_{n+1}) = X_k(\tau_n) + \delta_{k,\sigma_{n+1}}.$$

The initial conditions, the jump times τ_n, and the jump indices σ_n are enough to specify the system completely; knowing the τ_n and the σ_n tells us which motor jumps and when, and $Y(t)$ is constrained to follow (1) between jumps. In the analysis below another quantity will be useful, namely the times at which the kth motor jumps. We will denotes those by $\tau_{j,k}$, i.e.

$$\tau_{j,k} \text{ is the time at which the } k\text{th motor made its } j\text{th jump } (k = 1, \ldots, K,\ j \in \mathbb{N}). \tag{5}$$

Summarizing: When the system is in any given state, we choose the time of the next jump from the distribution (4), integrate $Y(t)$ according to (1) until this jump occurs, use (3) to determine which motor jumps, then repeat.

2.3 Regularity in the heavy cargo limit

We consider the model explicated above in the limit $\epsilon \to 0, \gamma \to \infty$, for some fixed K. This corresponds to having a fixed number of motors pulling an heavy cargo and assuming that the temperature effects are small. We show that in situations like these the motion becomes completely regular: the positions of the motors are all the same, they hop all together at fixed time intervals, and the cargo follows them according to (1). This result is stated precisely in Theorem 1 below. This result will also be relevant to explain the behavior of Kolomeisky-Fisher's model of myosin V described in section 3.1.

Let us first consider $K = 1$. We then have that $x = x_1$ jumps with intensity $\lambda(x - y)$, and y relaxes on a timescale of order γ. The expected amount of time until x jumps is $(\lambda(x - y))^{-1}$. Formally equating these two timescales gives

$$e^{\Delta V(x-y)/\epsilon} = \gamma,$$

or

$$\Delta V(x-y) \asymp \epsilon \log \gamma.$$

If $f(\cdot)$ is monotone increasing, so is $\Delta V(\cdot)$. So consider the limit

$$\epsilon \to 0, \quad \gamma \to \infty, \quad \epsilon \log \gamma \to \beta, \tag{6}$$

with $\beta > 0$, and set $z^\star > 0$ so that $\Delta V(z^\star) = \beta$. Notice that in the limit (6)

$$\begin{cases} \lambda(x-y) \ll \gamma, & \text{if } x-y > z^\star, \\ \lambda(x-y) \gg \gamma, & \text{if } x-y < z^\star. \end{cases}$$

This means that, when $x-y > z^\star$, the "jumping timescale" for the motor is much longer than the "relaxation timescale" for the cargo, i.e. we expect to see the cargo move an $O(1)$ amount before there is any jumping. When $x-y < z^\star$, these timescales are reversed, and we expect to see the motor jump before the cargo can relax appreciably. Putting all of this together, the total dynamics should be as follows. The cargo relaxes until the separation between the cargo and the motor is $z^\star$, at which time the motor jumps forward one step and things start over again. Theorem 1 below confirms this intuition.

The case with $K > 1$, but fixed, is not much more complicated. For each $m \in \mathbb{Z}$, we denote the number of motors at position $x = m$ as

$$K_m = \#(k \in \{1, \dots, K\} \,|\, x_k = m), \qquad \sum_{m \in \mathbb{Z}} K_m = K. \tag{7}$$

Notice that the leftmost motor is exponentially more likely to jump than any others because

$$\frac{\lambda(x_k - y)}{\lambda(x_l - y)} \asymp e^{-(x_k - x_l)/\epsilon}.$$

Thus, after some transients, we expect to be in the case where, for some m, $K_m \geq 0$, $K_{m+1} \geq 0$, but $K_j = 0$ for $j \notin \{m, m+1\}$. Without loss of generality, we assume that $m = 0$ and $y < 0$. Then (1) becomes

$$\frac{dy}{dt} = \gamma \left(K_0 f(-y) + K_1 f(1-y) \right),$$

but for finite K this still scales like γ. Moreover, although there may be some motors at $x = 1$, the intensity for a motor at $x = 0$ is still

$$\exp(-\Delta V(-y)/\epsilon),$$

and so matching timescales with K motors only affects the location of the distinguished jumping point, $z^\star$, by a term of size $\epsilon \log K$, which is negligible in the limit (6).

In other words, this suggests that all of the motors go to one point and wait there while the cargo relaxes. When the separation between the motors and the cargo reaches the distinguished value $z^\star$, all of the motors jump at once one step to the right. This makes the separation $z^\star + 1$, and the process repeats as the cargo relaxes toward $z^\star$.

The statements above can be made precise as the following

Theorem 1 *Define $\gamma(\epsilon)$ so that (6) holds, and consider the process $(X(t), Y(t))$ described above with initial condition $(X(0), Y(0))$, with parameters $\epsilon, \gamma = \gamma(\epsilon)$, and fixed K. Rescale time by $\gamma(\epsilon)$, and consider the process*

$$(\tilde{X}(t), \tilde{Y}(t)) = (X(t/\gamma(\epsilon)), Y(t/\gamma(\epsilon)))).$$

Denote the jump times of the kth motor in the rescaled process by $\widetilde{\tau}_{j,k} = \tau_{j,k}/\gamma(\epsilon)$, let $z^\star$ be the solution of $\Delta V(z^\star) = \beta$, and let $T^\star$ be the rescaled time the cargo takes to relax from being $z^\star + 1$ to $z^\star$ away from the motors, assuming that that they are all at the same positions, i.e.

$$\varphi_{\mathbf{0}, T^\star \gamma(\epsilon)}(z^\star + 1) = z^\star. \tag{8}$$

Then there exist $j^\star > 0$ such that for any $n \in \mathbb{N}$ and $h > 0$,

$$\lim_{\epsilon \to 0} \mathbb{P}\left(\sup_{1 \le k \le K} \sup_{j^\star \le j \le j^\star + n} |\widetilde{\tau}_{j+1,k} - \widetilde{\tau}_{j,k} - T^\star| > h \right) = 0, \tag{9}$$

In addition, for every k, there exists $j^{\star\star}(k) \in \mathbb{Z}$ such that for any $n \in \mathbb{N}$ and $h > 0$,

$$\lim_{\epsilon \to 0} \mathbb{P}\left(\sup_{1 \le k \le K} \sup_{j^{\star\star} \le j \le j^{\star\star} + n} \left|\widetilde{\tau}_{j,1} - \widetilde{\tau}_{j+j^{\star\star}(k),k}\right| > h \right) = 0. \tag{10}$$

The proof of Theorem 1 is given in the Appendix. (9) says that, after a transient period (accounted for by $j^\star$), the motors jump after waiting precisely a time $T^\star$ at each position along the track, i.e. we have regularity. (10) says that, after a transient period (which could differ for different motors, as accounted by $j^{\star\star}(k)$), they all jump precisely at the same time, i.e. we have synchrony. Notice that, by construction, the time $T^\star$ in the theorem depends on β but is is independent of $\gamma(\epsilon)$ and ϵ. Notice also that the result of the theorem holds for any force $f(\cdot)$ as long as it monotone increasing and the only impact of $f(\cdot)$ is to influence the rate of convergence in (9) and (10).

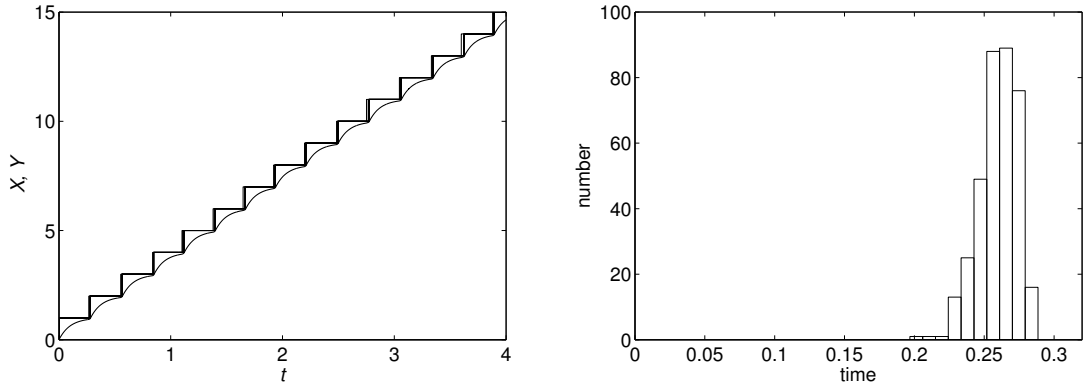

Figure 2: Trace and histogram for simulations of the system described here, with $N = 10$. We have chosen $\epsilon = 6.43 \times 10^{-2}$, $\gamma = 10^4$ and the results are shown in the rescaled time used in Theorem 1. The left frame shows dynamics quite close to the limit described in the theorem; all of the motors jump at about the same time, and the time between the set of motors jumping is nearly constant. The right frame shows a histogram of the random variable $\widetilde{\tau}_{10(k+1)} - \widetilde{\tau}_{10k}$; the theorem predicts that in the limit, this distribution should be a delta function at $T \approx 0.2727$. The real histogram looks close to a delta function: it has mean .2572 (an error of 5.7% from the limiting mean) and standard deviation 1.34×10^{-2} (giving a coefficient of variation of 5.2%).

2.4 Synchronization in the large population limit

In this section, we consider the model described above, but now consider the limit $\epsilon \to 0$, $K \to \infty$, for γ either fixed, or growing slowly enough that $\epsilon \log \gamma \to 0$. This corresponds to having a cargo, possibly heavy but much lighter than $e^{\epsilon^{-1}}$, pulled by many motors. In situations like these, we show that the jumps cluster in a different way: a small subpopulation of the motors step forward first, and once a critical number of these do so, the rest of the population undergoes a cascade. This subpopulation is small enough so that it is a negligible proportion of the whole population in the limit, but large enough that there is a law of large numbers effect and the time it takes for subpopulation to jump forward is deterministic in the limit.

Since $\epsilon \log \gamma \to 0$, as long as $\Delta V(x_k - y) > 0$, we have $\gamma / e^{\Delta V(x_k - y)/\epsilon} \to 0$ as $\epsilon \to 0$. This means that the cargo will attain its equilibrium position long before any motor with $x_k - y > 0$ jumps forward. We will

show below that the most important events in the dynamics occur on long timescales specified by the jumps of the motors with $x_k - y > 0$. This guarantees that, in the limit, y is always at its equilibrium position. In fact, this is consistent and justifies the equilibrium assumption in Duke's model [7].

In contrast to the last section, we will assume that the force f is linear for the purposes of simplicity, $f(z) = z$. This implies that

$$\Delta V(z) = z + \tfrac{1}{2}.$$

Note that a linear coupling is what is used in the full muscle contraction model in Section 3.2, so is sufficient for our purposes. Also note that there is no theoretical obstruction to extending the analysis below to nonlinear coupling.

As before, we restrict our attention to those configurations where, for some m, $K_m \geq 0$, $K_{m+1} \geq 0$, and $K_j = 0$ for all $j \notin \{m, m+1\}$, where K_m is the number of motors at position $x = m$ as defined in (7). The particular transition we are interested in understanding is the one in which initially we have $K_m = K$, $K_{m+1} = 0$, and transition to the situation where $K_m = 0$, $K_{m+1} = K$: in fact, we will show below that all transitions proceed this way, i.e. all the motors are at the same position, then they all jump by one step forward in some predictable way to the next position along the track, and the process repeat. Without loss of generality, it suffices to consider $m = 0$.

First, assume that after n jumps, the cargo is in the equilibrium position, i.e. $y = n/K$. Then

$$\Delta V(0, y) = \frac{1}{2} - y = \frac{1}{2} - \frac{n}{K}.$$

If $n < K/2$, $\Delta V(0, y) > 0$, so that

$$e^{\Delta V(0,y)} \gg \gamma.$$

In this case, the time it takes to jump is much longer than the time it takes to relax. Now, assume that the cargo is to the left of its equilibrium position. Then the time to jump is even longer, and in any case we can assume that the cargo attains its equilibrium position. Thus, for any $n < K/2$, the mean time to make the $(n+1)$st jump, $\mathbb{E}(\tau_{n+1} - \tau_n)$, is μ_n^{-1}, where

$$\mu_n = (K - n)e^{-1/2\epsilon}e^{n/K\epsilon}\left(1 + O\left(e^{-1/\epsilon}\right)\right).$$

For $n > K/2$, $\mu_n \geq O(1)$, making $\mathbb{E}(\tau_{n+1} - \tau_n) \leq O(1)$, independently of γ. In particular, the timescale of the first half of the events clearly dominates that of the second half. More precisely, if we rescale the time of this process by the constant prefactor $e^{1/2\epsilon}$, then the second half of the events will take a negligible amount of time.

This argument suggests that in the limit we are considering, it is equivalent to consider the process where we have replaced (1) with the condition that the cargo is always at equilibrium. It also suggests that the time that the entire jump sequence takes will be dominated by the early events and that the later events will be negligible in the limit. We make this more precise in the following theorem.

Theorem 2 *Assume that all the motors are at position $x = 0$ at time $t = 0$. Define*

$$\widetilde{\tau}_n = \epsilon^{-1}e^{-1/2\epsilon}\tau_n,$$

where τ_n are the jump times of the process as defined in Section 2.2. Consider any limit on ϵ, γ, K where

$$\epsilon \to 0, \quad K \to \infty, \quad \epsilon K \to \infty, \quad \epsilon \log \gamma \to 0.$$

Then, for any $p \in \mathbb{N}$, after pK steps, all the motors are at position $x = p$ almost surely in the limit and the time this took satisfies

$$\widetilde{\tau}_{pK} \to p \text{ almost surely} \tag{11}$$

In addition, for any $\alpha \in [0, 1)$ and $p \in \mathbb{N}$, let

$$n^\star = \arg\min_n \widetilde{\tau}_{n+pK} \geq \alpha + p.$$

be the number of jumps occurring during the time interval $[p, p+\alpha]$ *in one cycle. Then*

$$\frac{n^\star}{\epsilon K} \to \log(1-\alpha)^{-1} \text{ almost surely,}$$

and thus, for any $\alpha \in [0,1)$*,*

$$n^\star \to \infty, \quad \frac{n^\star}{K} \to 0, \text{ almost surely.}$$

Theorem 2 is also proved in the appendix. Notice that although it takes many steps ($n^\star \gg 1$) to start the chain-reaction which activates all of the motors, the proportion of motors which must jump to start this chain-reaction is arbitrarily small ($n^\star \ll K$). The correct picture is that some small subpopulation is activated, and that event causes the rest of the population to go forward. However, this subpopulation is also infinitely large in the limit, so that its effects become deterministic due to an effect similar to the Law of Large Numbers.

We again remark that whether we assume that the cargo relaxes continuously or moves to its equilibrium position instantaneously does not qualitatively affect the jump times in the limit. We will exploit this fact below in Section 3.2.

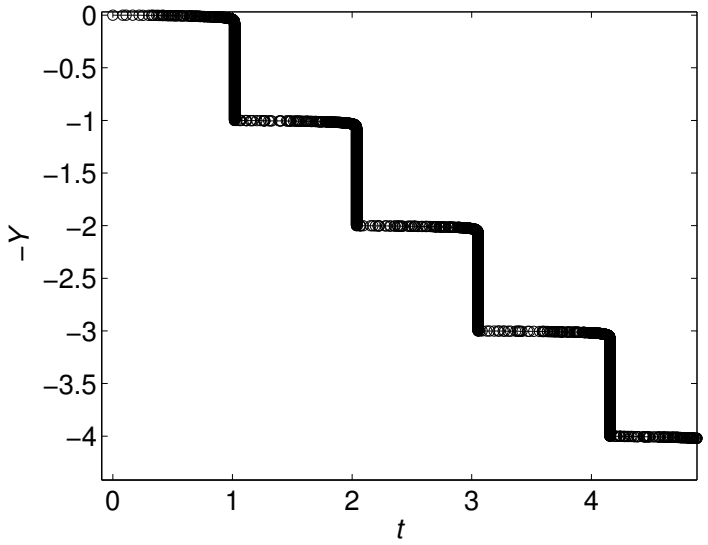

Figure 3: The position of the cargo for $N = 5000, \epsilon = 0.01, \gamma = 1$. We are graphing $-Y(t)$ instead of $Y(t)$ to make better the correspondence with figure 6 in Section 3.2. The position of the cargo at the time of the jump is represented by a circle: each time one motor jumps, the cargo moves by a step $1/N = 0.0002$. We can see that most of the jumps happen at the end, in a very short time. (According to the theorem, in the limit, a full proportion of these happen at the end in short time.) However, also notice that there are many events in the first part of the cycle as well, which is what gives regularity in the total time of the step.

Remark: Speed-up by staggering. Let us change the model described above slightly and assume that the landing sites of the motors are "staggered": choose some $\sigma \in [0,1)$ and say that the kth motor, instead of lying in $\mathbb{Z}$, has sites at $\mathbb{Z} + k\sigma/K$. One can do a similar analysis to that above, and the limiting motion we observe is different. In the model above, all of the motors sit at some m before the beginning of the burst; because of the staggering, the motors are now equally spread across the region $[m, m+\sigma]$. In particular, the equilibrium position of the cargo before the cascade is now $m + \sigma/2$, and moreover the equilibrium position of the motor after the nth jump is also shifted by $\sigma/2$. The net effect is that this changes the timescale of

the entire process from $e^{1/2\epsilon}$ to $e^{(1-\sigma)/2\epsilon}$, speeding up the entire cascade by the exponentially-large factor $e^{\sigma/2\epsilon}$.

As we will see in section 3.2, the realistic model of muscle contraction has, for some parameters, the property that the myosin heads land in a staggered fashion. This leads to a quicker cascade by the phenomenon described above.

3 Regularity and synchrony in realistic models of motor proteins

In this section, we analyze some realistic models of motor proteins and show that their behavior in biologically-relevant parameter ranges is similar to the limits analyzed in section 2.

In Section 3.1, we study the Kolomeisky-Fisher model for a processive molecular motor. It has been observed in numerical studies [21] of this specific model that the gait of this motor can be made very regular by coupling it to a heavy cargo. We show that this regularity can be explained by the limiting behavior described in section 2.3. The only difference here is that Kolomeisky-Fisher model adds the possibility of stepping backward; this leads to a new type of regular dynamics which we call "stuttering".

In Section 3.2 we analyze a cross-bridge model for muscle contraction due to Duke [7]. One salient feature of this model is its synchrony, specifically, that most of the motors act simultaneously, or nearly simultaneously. We show that this synchrony is the same as the limiting phenomena described in section 2.4.

3.1 Kolomeisky-Fisher model of Myosin V

In this section, we describe the framework of the Kolomeisky-Fisher model for motor proteins [11, 12, 16] and the generalization of this model due to Schilstra and Martin [21].

First we describe the Kolomeisky-Fisher class of models. Here a motor protein moves along a track and binds at specific sites $x = \ell D, \ell \in \mathbb{Z}$. The model then supposes that to move from one binding site to an adjacent one, the protein undergoes N intermediate biochemical transitions and assumes a different configuration after each of these steps. These steps must be visited in order, i.e. if the protein is in state S_j, then it can move forward into state S_{j+1} or backward into state S_{j-1}. To move from one binding site to the next, the motor then moves through the states $S_0, S_1, \ldots, S_{N-1}, S_0$ in order. (We assume periodicity; when the molecule moves forward out of state S_{N-1} it moves into S_0.) All of the biochemical steps are reversible, and the molecule can walk backward by moving through these steps in reverse. Finally, the model assumes that for a fixed force on the motor, the system makes these transitions with Poissonian statistics. Kolomeisky and Fisher showed that such a model gives a very accurate reproduction of experimental data for kinesin [12] (with $N = 4$) and myosin V [16] (with $N = 2$) for appropriate choices of parameters, in the context of applying a *constant force* to the motor protein.

Schilstra and Martin extended this model by tethering this motor to a cargo which can relax in time, so that the force on the motor is a function of time. In particular, it now becomes important to specify whether the intermediate biochemical transitions correspond to displacements in space. Choose $d_1, \ldots, d_N$ with $\sum d_j = D$, and say that the position of the motor increases by distance d_j when the motor moves from state S_j to state S_{j+1} (and decreases by distance d_{j-1} when the motor moves from S_j to S_{j-1}). This is postulating that the steps in configuration space do correspond to steps in physical space, and in particular, have the effect of increasing the force applied to the motor when the motor makes a forward transition, even for the intermediate stages. (In fact, the structural picture of what is actually happening with the motor protein is a bit more complicated than the model we are presenting, but this does not affect the one-dimensional motion of the motor along the track. See [16] for details.)

The stepping probabilities are then set as follows: if we denote by F the force between the motor and

cargo, then for $j = 1, \ldots, N$ define

$$u_j(F) = u_j(0) \exp\left(-\psi_j \frac{FD}{k_B T}\right), \qquad w_j(F) = w_j(0) \exp\left(\omega_j \frac{FD}{k_B T}\right), \tag{12}$$

where $\sum_{j=1}^{N}(\psi_j + \omega_j) = 1$. In any small time Δt, the motor in state S_j jumps forward with probability $u_j(F)\Delta t$ and backward with probability $w_j(F)\Delta t$. As with the model considered in Section 2, if the force were constant, all steps would be taken with Poisson statistics.

As in Section 2, we will allow the cargo to relax so that between jumps, this force is a decreasing function of time. Denote x as the position of the motor and y the position of the cargo, and between jumps we let y evolve according to

$$\gamma \frac{dy}{dt} = F(x - y), \tag{13}$$

where as before F is a monotone increasing function of $x - y$. Letting y relax is exactly what allows the statistics of the jumps to be non-Poissonian, as in Section 2. We will see below that it is more convenient to change variables in (13) to obtain an ODE for F. Since F is a monotone function of y if x is fixed, it is possible to do so. Writing $F = \chi(z)$, where χ is a monotone function, we calculate

$$\frac{dF}{dt} = \gamma^{-1} h(F), \tag{14}$$

where $h(F) = F\chi'(\chi^{-1}(F)) < 0$ for $F > 0$.

Summarizing: The state of the motor is encoded by x, the position in space, and the state S_j, with $j \in \{0, \ldots, N-1\}$. The state determines the intensity to jump forward or backward using (12), and if in state S_j, we move forward by d_j if we jump forward and move backward by d_{j-1} if we jump backward. Between jumps, the cargo relaxes as in (14).

3.1.1 The case with one biochemical transition per step, $N = 1$

Let us first consider in detail the case where we choose $N = 1$. We will see that choosing $N > 1$ does not add any appreciable complexity. Also, the main difference between Kolomeisky-Fisher models and those considered in Section 2.3 are that we now allow backward steps.

In the case $N = 1$, there are no intermediate states, so that the motor steps forward or backward by the same distance D whenever a jump occurs. From (12), we have

$$u(F) = u(0) \exp\left(-\frac{\psi FD}{k_B T}\right), \quad w(F) = w(0) \exp\left(\frac{\omega FD}{k_B T}\right). \tag{15}$$

In figure 4 we show some simulations of the system (15), (14). In both frames, we have chosen $F(x) = \kappa x$, and

$$u(0) = 10^5, \quad \kappa = 5 \times 10^{-5}\text{N/m}, \quad \gamma = 5 \times 10^{-5}\text{kg/s}, \quad k_B T = 4 \times 10^{-21}\text{J}.$$

However, in the left frame we choose $w(0) = 4.6416 \times 10^{-9}$ and in the right we choose $w(0) = 1.29 \times 10^{-4}$.

In both cases that the system is quite regular, and the times between jumps are almost the same. In the top frame we see that there are almost no false steps, and the system never jumps backward. In contrast, in the bottom frame, the system undergoes many forward and backward transitions: in particular, notice that there is a great deal of overlap in the times when the motor is in two subsequent states.

From this it is evident that, at least for some choice of parameters, the coupled system can move quite regularly. We will analyze this using an asymptotic analysis very much like that of Section 2.3. Let us first

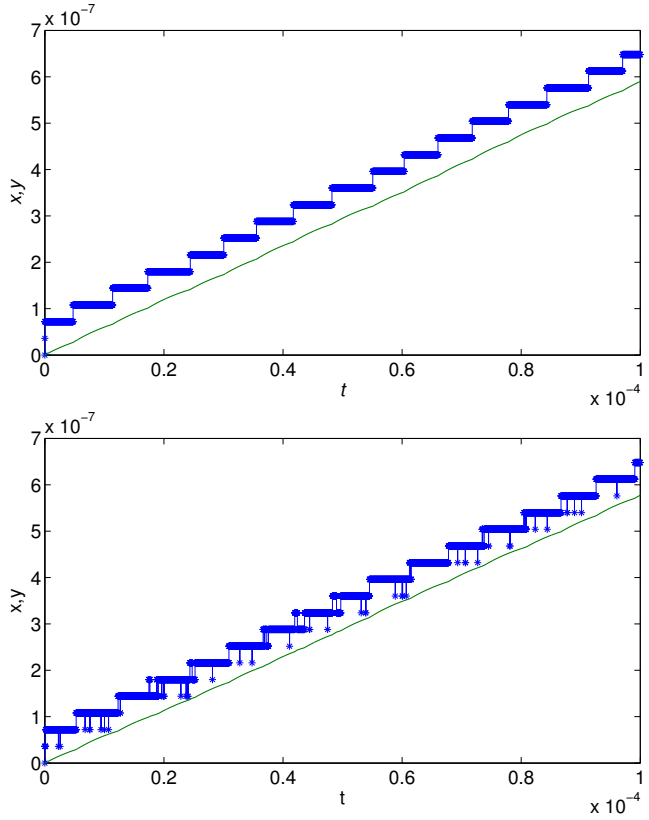

Figure 4: A simulation of the system (14), (15) for two sets of parameters as specified in the text. In each case, we represent the position of the motor with stars joined by straight lines, and the position of the cargo with a curve. In both case, the motion is very regular, but there is an important difference: in the bottom frame, the motor stutters at each step whereas it does not in the top frame.

compute the "stall force", i.e. the force at which a forward and a backward step are equally likely. Thus we choose F^{s} so that $u(F^{\mathsf{s}}) = w(F^{\mathsf{s}})$. Solving, we obtain

$$F^{\mathsf{s}} = \frac{k_B T}{D} \log\left(\frac{u(0)}{w(0)}\right).$$

We will be considering the small noise limit, so that $k_B T$ will be small. We also want to consider a scaling where F^{s} stays constant, and to do so we are required to take $u(0)/w(0) \to \infty$. We denote

$$\epsilon^{-1} = \log\left(\frac{u(0)}{w(0)}\right).$$

We now rescale (15) using F^{s} as our unit, i.e. set GF/F^{s}, giving

$$u(G) = u(0)\exp(-\psi G/\epsilon), \quad w(G) = w(0)\exp(\omega G/\epsilon).$$

We can also rescale time to get rid of one of the prefactors above; we choose to remove $u(0)$, so we rescale time as $\tau = u(0)t$. Using this rescaling and the fact that $\psi + \omega = 1$, we can rewrite these as

$$u(G) = \exp((\omega - 1)G/\epsilon), \quad w(G) = \exp((\omega G - 1)/\epsilon).$$

After time rescaling (14) reads

$$\frac{dF}{d\tau} = -\frac{\kappa}{\gamma u(0)} h(F) =: -\delta h(F), \tag{16}$$

and since $G = F/F^{\mathsf{s}}$, we obtain

$$\frac{dG}{d\tau} = -\delta F^{\mathsf{s}} h(G/F^{\mathsf{s}}).$$

Inspired by the analysis of Section 2.3, we will consider a limit where $\epsilon, \delta \to 0$. As in that example, we saw that the critical turnaround occurs when the jumping timescale equals the relaxation timescale, so we consider the limit where

$$\epsilon \to 0, \quad \delta \to 0, \quad \epsilon \log \delta^{-1} \to \beta, \quad \beta \in \mathbb{R}. \tag{17}$$

Once β is chosen, we define $G^{\mathsf{L}}, G^{\mathsf{R}}$ as

$$u(G^{\mathsf{R}}) = \delta, \quad w(G^{\mathsf{L}}) = \delta,$$

and we solve to obtain

$$G^{\mathsf{R}} = \frac{\beta}{1-\omega}, \quad G^{\mathsf{L}} = \frac{1-\beta}{\omega}.$$

We want to consider only those cases where $G^{\mathsf{R}} < 1$, so we constrain $\beta \in (0, \beta_{\mathsf{max}})$, where $\beta_{\mathsf{max}} = (1-\omega)$. We compute that, in the limit (17), the system satisfies

$$\begin{cases} u(G) \ll \delta, w(G) \ll \delta, & G \in (G^{\mathsf{R}}, G^{\mathsf{L}}), \\ u(G) \gg w(G), u(G) \gg \delta, & G < G^{\mathsf{R}}, \\ u(G) \ll w(G), w(G) \gg \delta, & G > G^{\mathsf{L}}. \end{cases}$$

Then in a similar manner to the example in Section 2.3, the system will always jump forward if $G < G^{\mathsf{R}}$, will always jump backward if $G > G^{\mathsf{L}}$, and will do neither, but relax under the dynamics of (16), for $G \in (G^{\mathsf{R}}, G^{\mathsf{L}})$. (The proof of this is almost exactly the same as for the analogous statements in Section 2.)

What happens after a jump? In the x variables, a jump corresponds to the motor moving forward a distance D. In the G variables, if we have $G = G^{\mathsf{R}}$ before a jump, then

$$x = \chi^{-1}(F^{\mathsf{s}} G^{\mathsf{R}}),$$

so G after the forward jump is

$$(F^{\mathsf{s}})^{-1} \chi(D + \chi^{-1}(F^{\mathsf{s}} G^{\mathsf{R}})),$$

and we can define the nondimensional constant

$$\zeta = (F^{\mathsf{s}})^{-1} \chi(D + \chi^{-1}(F^{\mathsf{s}} G^{\mathsf{R}})) - G^{\mathsf{R}}.$$

This is complicated only because the force is nonlinear. It is easy to see that in the simplest case of $\chi(x) = \kappa x$, then

$$\zeta = \kappa D / F^{\mathsf{s}}.$$

If $G^{\mathsf{R}} + \zeta < G^{\mathsf{L}}$, the dynamics are very similar to the case in Section 2.3 where there is no backward jumping. After the jump, the total intensity to jump is much less than δ, so we expect relaxation. As before, G relaxes until $G = G^{\mathsf{R}}$, at which time the jumping timescale again becomes shorter than the relaxation timescale, and we repeat.

If $G^{\mathsf{R}} + \zeta > G^{\mathsf{L}}$, something additional happens. If the motor jumps forward when $G = G^{\mathsf{R}}$, then immediately after the jump, $G > G^{\mathsf{L}}$. Because of this, immediately after the jump we have $w(G) \gg \delta$, meaning that the timescale of jumping backward is much shorter than relaxation, so we expect to jump backward before the cargo can relax. But, of course, immediately after we jump backward, G is again less than G^{R}, and so we jump forward again, and so on. We call this situation "stuttering" because the motor bounces back and forth many times before the cargo moves any appreciable amount.

The stuttering phase does not last forever. Although the cargo oscillates between two states, each of these states lies to the right of the cargo (since $G^{\mathsf{R}} > 0$), so that the cargo will always feel a rightward force, and will continue to relax to the right. We will remain in the stuttering state as long as the value of G after the forward jump is greater than G^{L}, or, the value of G before the jump is less than $G^{\mathsf{L}} - \zeta$. So, let us assume that $G^{\mathsf{L}} - \zeta > 0$. This gives three regions in G under which we get three types of behavior. For $G \in (G^{\mathsf{R}}, G^{\mathsf{L}})$, the cargo relaxes and G decreases slowly. For $G \in (G^{\mathsf{L}} - \zeta, G^{\mathsf{R}})$, the motor stutters between two states, and the cargo continues to relax. Then once G reaches $G^{\mathsf{L}} - \zeta$, it jumps to G^{L} and does not jump back, and the cycle continues anew.

To compute the dynamics of the cargo while the motor is stuttering, we simply need to compute the relative proportion of time the motor spends on the front end, or the back end, of the stuttering pair. It is easy to see that if we set

$$\rho = \rho(G, \zeta) = \frac{u(G)}{u(G) + w(G + \zeta)}, \text{ for } G \in (G^{\mathsf{L}} - \zeta, G^{\mathsf{R}}),$$

the motor spends a proportion of time equal to ρ in the forward state. Then (16) becomes

$$\frac{dG}{d\tau} = -\delta\rho G - \delta(1-\rho)(G+\zeta) = -\delta(G + (1-\rho)\zeta).$$

Moreover, we see that $\rho \to 0$ as $G \to G^{\mathsf{R}}$, and $\rho \to 1$ as $G \to G^{\mathsf{L}} - \zeta$.

We also remark that it is possible that the system can never make it out of a stuttering state, if ζ is sufficiently large.

In summary, we have two cases, depending on ζ, with or without stuttering. If $\zeta < G^{\mathsf{L}} - G^{\mathsf{R}}$, there is no stuttering and the dynamics are as in Section 2.3: in the G variables, the system relaxes to G^{R}, jumps to $G^{\mathsf{R}} + \zeta$, and repeats. Of course, each of these periods corresponds to the motor moving forward D in space. From this we can compute the period in the rescaled time, which is

$$\delta^{-1} \log\left(\frac{G^{\mathsf{R}} + \zeta}{G^{\mathsf{R}}}\right).$$

In the original time, this equals

$$T = \kappa\gamma^{-1} \log\left(\frac{G^{\mathsf{R}} + \zeta}{G^{\mathsf{R}}}\right).$$

Of course, the velocity of the complex is then D/T.

If $\zeta > G^{\mathsf{L}} - G^{\mathsf{R}}$, there is stuttering and we can do the same calculation to compute the period.

We can understand the boundary between the two phases as follows. If we consider β tunable (we can change β by modifying the ratio of $u(0)$ and $w(0)$), we see that the critical value of ζ at which stuttering sets in is

$$\zeta_{\mathsf{crit}}(\beta) = G^{\mathsf{L}} - G^{\mathsf{R}} = \frac{1 - (\beta + \omega)}{\omega(1-\omega)}.$$

This moves in opposite sign to β, reaching zero at β_{max}. In particular, if we hold all other parameters fixed by increasing β, the system is more likely to stutter.

3.1.2 The case with multiple biochemical transitions per step, $N > 1$

There is no appreciable complexity added when $N > 1$. We do the same sort of nondimensionalization as done in the previous section. For each j, we can compute the stall force at the jth step to be

$$F_j^{\mathsf{s}} = \frac{k_B T}{D(\omega_j + \psi_j)} \log\left(\frac{u_j(0)}{w_j(0)}\right).$$

We again rescale space by F_j^{s} to obtain

$$u_j(G_j) = u_j(0) \exp\left(-\frac{\psi_j}{\omega_j + \psi_j}\frac{G_j}{\epsilon_j}\right), \quad w_j(G_j) = w_j(0) \exp\left(\frac{\omega_j}{\omega_j + \psi_j}\frac{G_j}{\epsilon_j}\right),$$

where

$$\epsilon_j^{-1} = \log\left(\frac{u_j(0)}{w_j(0)}\right).$$

Rescaling time by $u_j(0)$ and writing $\alpha_j\omega_j/(\omega_j+\psi_j)$ gives

$$u_j(G_j) = \exp((\alpha_j - 1)G_j/\epsilon_j), \quad w_j(G_j) = \exp((\alpha_j G_j - 1)/\epsilon),$$

and the evolution equations become

$$\frac{dG_j}{d\tau_j} = -\delta_j F^{\mathsf{s}} h(G_j/F^{\mathsf{s}}).$$

As before, we consider the limit when

$$\epsilon_j \to 0, \quad \delta_j \to 0, \quad \epsilon_j \log \delta_j^{-1} \to \beta_j.$$

We can again compute $G_j^{\mathsf{L}}, G_j^{\mathsf{R}}$ by $u_j(G_j^{\mathsf{R}}) = \delta_j, w_j(G_j^{\mathsf{L}}) = \delta_j$, and solving gives

$$G_j^{\mathsf{R}} = \frac{\beta_j}{1-\alpha_j}, \quad G_j^{\mathsf{L}} = \frac{1-\beta_j}{\alpha_j}.$$

Again, we constrain $\beta_j \in (0, 1-\alpha_j)$. As before, the system always jumps forward if $G_j < G_j^{\mathsf{R}}$. To compute what happens after the jump is similar to that in the previous section, and in fact we have that after a forward jump from G_j^{R}, we have

$$G_{j+1} = (F_{j+1}^{\mathsf{s}})^{-1}\chi(d_j + \chi^{-1}(G^{\mathsf{R}}F_j^{\mathsf{s}})),$$

and in the particular case where $\chi(x) = \kappa x$, we get

$$G_{j+1} = \frac{F_j^{\mathsf{s}}}{F_{j+1}^{\mathsf{s}}}G^{\mathsf{R}} + \frac{\kappa d_j}{F_{j+1}^{\mathsf{s}}}.$$

Thus, after a forward jump out of the jth stage, we jump into the $j+1$st stage with this initial condition. As in the case $N=1$ we can compute whether or not the $j \to j+1$ transition stutters by checking whether the new G_{j+1} is greater than G_{j+1}^{L} or not, but the analysis is very similar to the previous case so we omit it here.

It was shown in [16] that a $N=2$ model matches experimental data for myosin V quite well. In [21], a numerical simulation was carried out which coupled this type of stochastic stepper to a heavy cargo. It was shown empirically that the gait of the myosin V molecule becomes quite regular in a parameter regime which is consistent with biologically-relevant parameters. See Figure 3 of [21], and in particular compare the bottom right frame of that figure to Figure 4 here. For various values of parameters, [21] observed both stuttering and non-stuttering behavior.

3.2 Duke model of Myosin II

We use a slight modification of Duke's model in [7]. This model describes the mechanochemical cycle of myosin II in the context of muscle contraction. The mechanism for muscle contraction is the relative motion of a myosin II filament with an actin filament in the sarcomere, and the work to perform this relative sliding is achieved under an actin-activated ATPase cycle [1]. The many heads of the myosin II molecule act as the stochastic motors considered above, and one particularly interesting outcome of the numerical simulations in [7] is the synchronization of the action of these motors: the model undergoes phases where all, or almost all, of the motors pull at the same time. As we showed in Section 2.4, many motors working in parallel can lead to synchronization in certain scaling limits. We will show below that the phenomenon observed in one phase of the motion of the myosin complex in Duke's model is explained exactly by the scaling limit chosen above.

The model is as follows: there are two filaments, which we call the upper and lower filaments. The upper filament represents the myosin II filament, and the lower the actin filament. The myosin heads are always attached to the upper filament, and the point of attachment does not change; however, they can detach, and reattach, to the lower filament at any time or at any point in space. Moreover, we assume that the upper filament is immobile and any force applied between the two filaments will cause the lower filament to slide. See Figure 5, based on Figure 1a of [7].

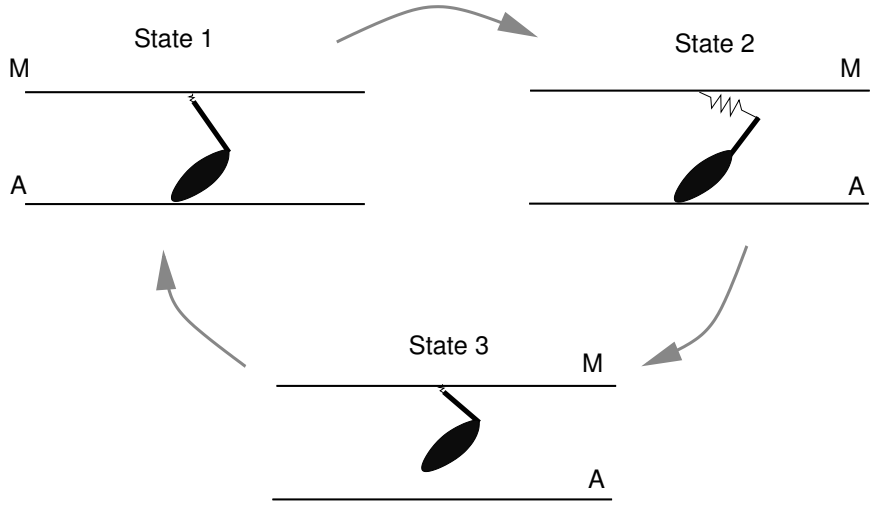

Figure 5: A schematic diagram of the three stages used in [7]. The model represents three states for any myosin head. If the motor is attached but not extended, it can extend and increase the applied force. If attached and extended, it can detach, and detached heads can reattach stochastically. This diagram suggests the physical reasoning behind the rates chosen in (19), the first two transitions correspond to stochastic extension of an elastic element beyond an energy barrier, and in particular depend on the force applied between the two filaments.

We denote by u_k the position of the connection of the kth myosin head to the upper filament, and by y the total displacement of the lower filament with respect to the upper filament. We choose some distinguished point on the lower filament which we denote as $x = 0$. We denote the point of connection between the kth myosin head and the lower filament as x_k, and this is relative to the distinguished point $x = 0$. If the lower filament has changed position, the actual position in space of the connection between the kth myosin head and the lower filament will lie at $x_k + y$.

Under the swinging lever hypothesis, each myosin molecule can lie in one of three states; the state determines the force the lower filament feels:

1. attached and unextended, force $= -\kappa(x_k - u_k + y)$,
2. attached and extended, force $= -\kappa(x_k - u_k + y + d)$,
3. detached, no force.

If we denote the set of indices of molecules in state j by S_j and the denote the size of this set by K_j, then we can see that the total force exerted can be written as

$$-\kappa \left(\sum_{k \in S_1 \cup S_2} (x_k - u_k + y) + K_2 d \right) + F.$$

Assuming that the lower filament is always at equilibrium position gives

$$y = \frac{Q - K_2 d - \sum_{k \in S_1 \cup S_2} (x_k - u_k)}{K_1 + K_2}, \tag{18}$$

where we write $Q = F/\kappa$. As we showed in Section 2.4, whether we assume the cargo relaxes instantaneously or not does not greatly affect the dynamics; we could replace (18) with an ODE much like (1) and we would obtain similar dynamics in the large population limit.

As for the transitions, Duke [7] assumes that transitions are exponentially distributed with non-constant rates. More precisely, both the $S_1 \to S_2$ and $S_2 \to S_3$ transitions are modeled by escape from a potential well. We thus have

$$\begin{aligned} s_k = 1, \quad & \lambda_k^{(1)} = \exp(-(\Delta G_{\mathsf{stroke}} + \kappa d(2x+d))/2k_BT), \\ s_k = 2, \quad & \lambda_k^{(2)} = k^0_{\mathsf{ADP}} \exp(-\kappa\delta(x+d)/2k_BT), \\ s_k = 3, \quad & \lambda_k^{(3)} = k_{\mathsf{bind}}. \end{aligned} \tag{19}$$

We choose as our small parameter

$$\epsilon = \frac{\kappa d^2}{k_B T},$$

and from this we see that

$$\begin{aligned} \lambda_k^{(1)} &= \exp(-\Delta G_{\mathsf{stroke}}/k_BT)\exp(-(x+d/2)/d\epsilon), \\ \lambda_k^{(2)} &= k^0_{\mathsf{ADP}} \exp(-\delta(x+d)/d\epsilon). \end{aligned}$$

In particular, $\lambda_k^{(1)}$ has exactly the same form as the Poisson intensities in Section 2.4.

We first compute the change in position of the lower filament given that the molecule indexed by k^* makes a transition. We write $K_a = K_1 + K_2$, and then

$$\begin{aligned} 1 \to 2, \quad & y \mapsto y - \frac{d}{K_a}, \\ 2 \to 3, \quad & y \mapsto \frac{K_a y + (x_{k^*} - u_{k^*} + d)}{K_a - 1}, \\ 3 \to 1, \quad & y \mapsto y. \end{aligned}$$

Clearly, whenever a molecule extends, the force on the lower filament increases and so it moves to the left. Whenever a molecule detaches, the force on the lower filament decreases, so it moves to the right. The dynamics are somewhat complicated by the fact that the magnitude of these changes depends on the state of the other molecules, in particular the number of molecules which are attached at the time of transition.

The total dynamics of the complex is as follows: as in Section 2.4, the system undergoes a bursting phenomenon where the majority of the motors extend in a short time. During this phase, the lower filament moves $O(d)$ to the left (and in particular moves exactly d if all molecules extend). After this, the majority of the system lies in state 2, and we expect to see many detachments, and then reattachments, before the system can reset itself. The crucial consideration is how far back to the right does the lower filament slide during the detachment and reattachment stage. For example, if it backslides more than d, then the probability of another bursting event where all of the myosin molecules extend becomes exponentially smaller, and we expect the system to stall. If it backslides significantly less than d, then the lower filament has made a net motion to the left and the muscle sarcomere has contracted. We can then expect the process to repeat.

What may be surprising is that the total amount of backsliding which occurs depends on the sequence of detachments and reattachments, in particular how they are collated. To show this, first assume for concreteness that we start the system in a state with all molecules in state 1, $x_k = u_k$ for all k, and $y = 0$. If we apply a force F, and then wait until all K myosin molecules extend, the lower filament will then lie at $y_0 = Q - d$.

We imagine the two extreme cases. The first is that the myosin molecules detach one-by-one, and before another can detach, the loose one always reattaches. The second is that all molecules but one detach, then all of these reattach. (Technically, the most extreme case is that all myosin molecules detach, but in this

case the applied force pushes the lower filament without anything to counter it, and we have $y = \infty$; the model breaks down.)

After one detachment, we have

$$y_1 = \frac{K(Q-d)+d}{K-1} = \frac{KQ+(1-K)d}{K-1} = \frac{K}{K-1}Q - d.$$

Reattaching the loose head does not change y, and thus after one detachment-reattachment pair, we have multiplied Q by the ratio $K/(K-1)$. Moreover, it is easy to see that repeating this process K times will give

$$y_K = \left(\frac{K}{K-1}\right)^K Q - d.$$

For K sufficiently large, this coefficient tends to e. Moreover, notice that the location of the reattachments will be staggered. In fact, we can solve exactly for the positions of the attachment to the lower filament of the myosin molecule which was the mth to reattach

$$x_k + y = u_k + \left[\left(\frac{K}{K-1}\right)^K - \left(\frac{K}{K-1}\right)^m\right] Q.$$

On the other hand, the other extreme is that we have $K-1$ detachments followed by $K-1$ reattachments. After the first detachment, we have

$$y_1 = \frac{K}{K-1}Q - d,$$

as before. But if we detach now, there are only $K-1$ motors attached, and thus we have

$$y_2 = \frac{(K-1)y_1 + d}{K-2} = \frac{KQ-(K-1)d+d}{K-2} = \frac{K}{K-2}Q - d.$$

It is easy to see that after k consecutive detachments, we have

$$y_k = \frac{K}{K-k}Q - d,$$

and thus $K-1$ detachments would give

$$y_{K-1} = KQ - d.$$

In the general case, the detachments and reattachments can happen in a wide variety of sequences. Denote by $\alpha(n)$ the number of reattachments we have taken place before the nth detachment. Of course, $\alpha(n) < n$, and in the two extreme cases above we chose $\alpha(n) = n-1$, or $\alpha(n) = 0$. Then, denoting

$$A = \prod_{n=1}^{K} \frac{K-\alpha(n)}{K-\alpha(n)-1},$$

we see that after the sequence of detachments and reattachments represented by $\alpha(n)$ we have

$$y = AQ - d.$$

The arguments above show that

$$e \le A \le K.$$

Now, as long as we choose $eQ < d$, there will be some sequences for which the filament backtracks less than it stepped forward during the burst. By decreasing Q, we increase the set of allowable sequences which do not lead to too much backstepping.

Moreover, A can be controlled by varying the parameters. For example, choosing k_{bind} sufficiently large makes $\alpha(n)$ very unlikely to be small. This has the joint effect of both decreasing A and staggering the locations where the molecules have landed on the lower filament. Thus there is less backsliding during the detachment-reattachment phase, and the staggering makes a forward cascade happen more quickly.

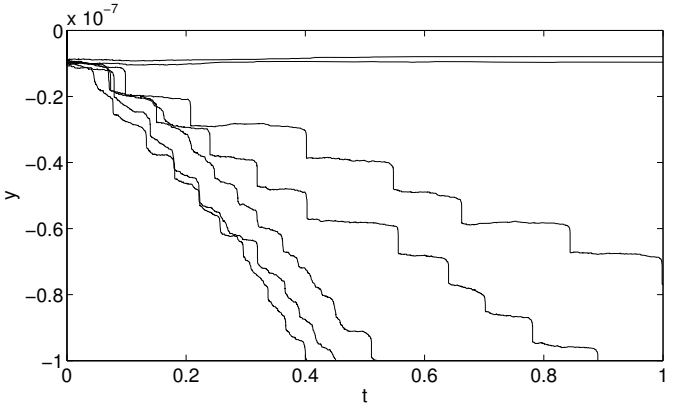

Figure 6: The is an example simulation of the model described here where we show $y(t)$, the position of the lower filament versus time, for various values of the applied force, ranging from 25 pN to 150pN. We see that for small applied forces, the lower filament moves with very little stalling or backstepping. For high values of the force, the lower filament completely stalls. There is an intermediate regime where the system undergoes synchronized pushes, separated by quiescent stages, similar to that seen in dynamics of the simpler model of Section 2.4 (compare to Figure 3).

4 Outlook and generalizations

We have considered a general class of stochastic models for networks of motor proteins and shown that, in particular scaling limits, these models display regularity and synchrony. We have further shown how this can explain observed behavior in numerical models of such systems. The results here, and their applicability in a larger scheme, suggest that there are simple organizing principles governing stochastic networks in a very general context and in biologically-applicable parameter regimes.

For example, we could follow the methodology of [18, 8] and model the motor by a Brownian ratchet. To be more concrete, consider the model in Section 2 with $K = 1$ and replace the motor with a point particle which diffuses in a tilted potential:

$$\begin{aligned} dX_k &= (-\nabla U(X_k) - f(X_k - Y))\, dt + \sqrt{2\epsilon}\, dW_k(t), \quad k = 1, \ldots, K \\ \gamma dY &= \sum_{k=1}^{K} f(X_k - Y)\, dt, \end{aligned} \tag{20}$$

where U is the sawtooth-like potential used for Brownian ratchets (see figure 7), and as before ϵ, γ are small. It is a standard result of large deviation theory [13] that in the limit $\epsilon \to 0$, the escape time past the potential jumps have statistics exactly the same as the Poisson jumping times used above in Section 2. It is easy to see that we will obtain the same results as above in this more complicated case. In particular, this can represent a massive simplification of models currently used; on first glance, such a model would be very complicated to analyze, as one would have to move to the Kolmogorov equations with many independent variables. However, with γ sufficiently large, this would allow an analysis very much like the one presented here to first average over the fast stochastic process and replace the detailed dynamics of the dX_k equation with a model like that in Section 2 encapsulating the jump times. The authors are currently studying a more detailed analysis of exactly such a system in [6]. This analysis confirms that regularity and synchrony is not tied to a specific model but rather is quite generic to a wide class of systems where the Arrhenius time-scale of jumping of the motors interplays in a nontrivial way with another slow time scale in the system. This analysis also give the tools to quantify the motion of these systems even in setting much more complicated than the models studied in the previous section, or the Brownian ratchet model (20) above, because it uses results from large deviation theory and matching timescale argument rather than a full analysis of the master

equation for the probability density of the system (which would be extremely complicated). In particular, there is hope to apply these ideas even to complicated models where the motor or the cargo or both have moving internal structures which participate to the motion of the compound.

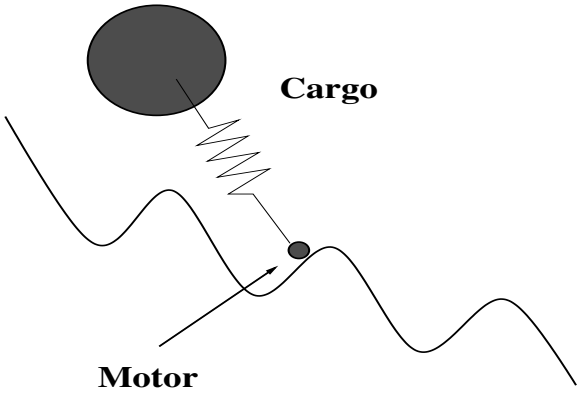

Figure 7: A schematic of the model described in (20) with $K = 1$. The motor is subject to the deterministic forces from both the potential and the tethered cargo, and also to the stochastic forcing from the white noise.

Another point worth making about our results is that we have done an analysis of systems which are not quite like those previously considered in experiments. The Kolomeisky-Fisher models have done an excellent job of explaining measurable quantities for motor proteins held at a constant force, but the present analysis shows that these systems can behave very differently when coupled to a relaxing cargo (and, in fact, this may be a better representation of the actual *in vivo* conditions under which these proteins operate). Thus, we make falsifiable predictions: as was noted in [21], coupling a motor protein molecule to a relaxing cargo can lead to regularity, but more quantitative statements are possible. In Section 3.1, our analysis can be used to predict many quantities, including the velocity of a regularly-stepping motor and the distance between motor and cargo which we expect to observe at the jump times. These predictions could be checked by experiments like [20] which are modified to include the relaxing cargo.

Finally, an interesting question is how these sorts of dynamics may be useful in real biological systems. As was pointed out in [21], regular behavior in a transporting motor can be useful for the reason that several such motors can now be strung serially into a single track without fear of collision and jamming. Regarding synchrony, it is pointed in [7] that it may explain certain types of oscillatory behavior of muscles subject to strong changes in cargo. Synchrony has also been proposed as a mechanism to explain observed direction-reversing behavior in certain motility assays of Ncd11 [3, 9]. We hope that the analysis above will offer a way to investigate further the viability of these explanations by allowing to test them against quantitative predictions for the models used to describe the protein motors.

Acknowledgements

The authors would like to thank Paul Atzberger, George Oster and Charles Peskin for illuminating comments and discussions during the course of this work. RELD was supported as a Courant Instructor at NYU, and EVE was supported in part by NSF grants DMS02-09959 and DMS02-39625, and by ONR grant N00014-04-1-0565..

A Proofs of Theorems 1 and 2

Proof of Theorem 1. We first show that, at some time $t > 0$, we have all of the components of $X(t)$ equal, namely $X_k(t) = X_l(t)$ for all k and l. The reason this is true is that the probability of a motor jumping

which is not the leftmost motor is exponentially small in ϵ. This means that with probability exponentially close to one, any time a motor jumps, it is the (or one of the) leftmost ones. For any initial condition, it only takes a finite number of jumps, where each is of the motor which is currently the leftmost, to put all motors in the same place. Therefore with probability exponentially close to one, we will have all motors in the same place at some time. This finite number of jumps is one way to obtain $j^\star > 0$ in the statement of the theorem.

Since the system is Markov, we can then assume without loss of generality that all the $X_k(0)$ are equal, and due to the translational invariance in the system, let us say $X_k(0) = 0$. We define $z(t) = -Y(t)$ and $z_0 = z(0)$; since $Y(t)$ evolves according to (1), for $t < \tau_1$, we will have that $Y(t)$ increases monotonically, and thus $z(t)$ decreases monotonically. We can then ask, for any $z_\mathsf{f} < z_0$, whether some $X_k(t)$ will jump before $z(t)$ reaches z_f, or, equivalently, if $z(\tau_1) > z_\mathsf{f}$. There is a unique $t = t(z_0, z_\mathsf{f})$ such that $\varphi_{\mathbf{0},t}(z_0) = z_\mathsf{f}$, and we can compute, from (4), that

$$\mathbb{P}_{z_0}(z(\tau_1) > z_\mathsf{f}) = 1 - \exp\left(-\int_0^{t(z_0,z_\mathsf{f})} K\lambda(\mathbf{0}, \varphi_{\mathbf{0},t}(A))\,dt\right).$$

Using (1) to change variables gives

$$\mathbb{P}_{z_0}(z(\tau_1) > z_\mathsf{f}) = 1 - \exp\left(-\int_{z_0}^{z_\mathsf{f}} \gamma K \frac{\lambda(z)}{f(z)}\,dz\right).$$

From (6) and (2) we have

$$\mathbb{P}_{z_0}(z(\tau_1) > z_\mathsf{f}) = 1 - \exp\left(-\int_{z_0}^{z_\mathsf{f}} K \frac{\exp(-\frac{\beta - \Delta V(z)}{\epsilon})}{f(z)}\,dz\right). \tag{21}$$

By assumption, $z_0 > z^\star$. Let us first assume that $z_\mathsf{f} > z^\star$ as well. Then we have that for all $z \in [z_0, z_\mathsf{f}]$, $z > z^\star$, or $\Delta V(z) > \beta$. Taking $\epsilon \to 0$, we see that the integrand then becomes exponentially small for all z in the domain of integration, meaning the integral is exponentially small, making the right-hand side of (21) arbitrarily small.

On the other hand, if $z_\mathsf{f} < z^\star$, then there are values of z in the domain for which $\Delta V(z) < \beta$, making the integral exponentially large, which makes the right-hand side of (21) arbitrarily close to one. Thus

$$\lim_{\epsilon\to 0, \gamma=\gamma(\epsilon)} \mathbb{P}_{z_0}(z(\tau_1) > z_\mathsf{f}) = \mathbf{1}(z_\mathsf{f} < z^\star), \tag{22}$$

and moreover the same argument as above shows that this limit is uniform for z_0 in any compact set. In particular, this probability does not depend on z_0 or on N. In the limit, the first jump time τ_1 is the time at which the separation between x and y is exactly $z^\star$, and we can compute this as

$$t(z_0, z^\star) = \int_{z^\star}^{z_0} \frac{\gamma d\zeta}{f(\zeta)}. \tag{23}$$

We can also restate (22) by saying that since f is smooth, for any $h > 0$,

$$\lim_{\epsilon\to 0, \gamma=\gamma(\epsilon)} \mathbb{P}_{z_0}(|\tau_1 - t(z_0, z^\star)| > h) = 0.$$

After the first jump, we have $K-1$ motors at $x = 0$ and one motor at $x = 1$. We know that with probability exponentially close to one, one of the motors at $x = 0$ will jump first. Moreover, to compute the time at which the next jump occurs, replace z_0 with $z^\star$ and K with $K - 1$ in (21), and we see that for any $z_\mathsf{f} > z^\star$, the second jump will have taken place before the cargo reaches $-z_\mathsf{f}$. Repeating this argument K times shows that in the limit, all K motors jump from $x = 0$ to $x = 1$ in arbitrarily small time if ϵ is sufficiently small. As thus we have

$$\lim_{\epsilon\to 0, \gamma=\gamma(\epsilon)} \mathbb{P}_{z_0}(|\tau_m - t(z_0, z^\star)| > h) = 0, \quad m = 1, \ldots, K.$$

As we continue, this process repeats itself: after a series of all K motors jumping, the cargo relaxes until the separation between cargo and the motors is $z^\star$, and then the motors jump one step forward. At this time, the separation is now $z^\star + 1$, and we repeat. Thus for any $\ell > 1$, the amount of time between $\tau_{\ell K}$ and $\tau_{(\ell+1)K}$ is given by

$$t(z^\star + 1, z^\star) = \int_{z^\star}^{z^\star+1} \frac{\gamma\, d\zeta}{f(\zeta)}.$$

Now consider the case where $Y(0) > -z^\star$. Consider (21) with $z_0 < z^\star$. By similar arguments, if we choose any $z_\mathsf{f} < z_0$, then the right-hand side of (21) is exponentially close to one. From this, we can see that in the limit (6), $\tau_1, \ldots, \tau_N$ are all equal to 0. If, after these jumps, $1 - Y(0) < -z^\star$, then the same argument implies that $\tau_{N+1}, \ldots, \tau_{2N}$ goes to zero in the limit as well. Repeat this argument until, for some m, $m - Y(0) \geq -z^\star$, and then apply the argument as above. □

Proof of Theorem 2. We will see that all we need to study is the dynamics of the beginning (or the head) of the sequence of $\widetilde{\tau}_n$ to get the estimates we need for (6).

We have

$$\widetilde{\tau}_n - \widetilde{\tau}_{n-1} = \frac{e^{-n/K\epsilon}}{\epsilon(K-n)}.$$

We will replace $\widetilde{\tau}_n$ with $\widehat{\tau}_n$, where we define $\widehat{\tau}_n - \widehat{\tau}_{n-1}$ to be exponentially-distributed with mean

$$\mathbb{E}(\widehat{\tau}_n - \widehat{\tau}_{n-1}) = (\epsilon K)^{-1} e^{-n/K\epsilon}.$$

To justify this approximation, notice that if we choose any m such that $m/N \to 0$ in the limit, we have

$$\sum_{n=0}^{m} \frac{e^{-n/K\epsilon}}{\epsilon K} \leq \sum_{n=0}^{m} \frac{e^{-n/K\epsilon}}{\epsilon(K-n)} \leq C_{K,m} \sum_{n=0}^{m} \frac{e^{-n/K\epsilon}}{\epsilon K},$$

with

$$C_{K,m} = \frac{K}{K-m}.$$

But $C_{K,m} \to 1$ and thus the two sequences have the same mean. However, we know all of the moments of $\widetilde{\tau}_n - \widetilde{\tau}_{n-1}$ and $\widehat{\tau}_n - \widehat{\tau}_{n-1}$, and thus we can make the same sandwiching argument for any of the moments. In any case, for any $\alpha(K)$ with $\alpha(K)/K \to 0$ as $K \to \infty$, we can replace the first $\alpha(K)$ terms in the hypergeometric sum with the first $\alpha(K)$ terms of the geometric sum, and the moments of these two random variables can be made arbitrarily close.

For simplicity we write $\nu = (\epsilon K)^{-1}$ below, noting that $\widehat{\tau}_n - \widehat{\tau}_{n-1}$ is distributed with mean $\nu e^{-k\nu}$. Consider the Markov process $X_\nu(t)$ with generator

$$L_\nu f(x) = \nu^{-1} e^x (f(x+\nu) - f(x)). \tag{24}$$

We will be taking the limit $\nu \to 0$, and in this limit the continuum approximation is given by

$$\dot{x} = e^x, \quad x(0) = 0. \tag{25}$$

Now, choose any $\beta > 0$. At what time does the process (24) reach β? Clearly, we must take $\beta\nu^{-1}$ steps to do so. After n steps, the rate is $\nu^{-1} e^{n\nu}$, meaning that the time before the next jump is given by an exponentially-distributed random variable with mean $\nu e^{-n\nu}$, the same distribution of $\widehat{\tau}_n - \widehat{\tau}_{n-1}$. The time at which we have taken $\beta K\epsilon$ jumps is then $\widehat{\tau}_{\beta K\epsilon}$, the quantity we are interested in.

So, now solve (25), the solution is

$$x(t) = \log\left(\frac{1}{1-t}\right).$$

Define $t_\beta = 1 - e^{-\beta}$ so that

$$x(t_\beta) = \beta.$$

Now, we apply Kurtz' theorem [13, 23]. For any $\epsilon > 0, T > 0$, there exist $C_1, C_2 > 0$ such that

$$\mathbb{P}\left(\sup_{t\in[0,T]} |X_\nu(t) - x(t)| \geq \epsilon\right) \leq C_1 e^{-C_2\epsilon^2\nu^{-1}}.$$

Applying the mean value theorem, and noting that $|\dot{x}| > 1$ gives that for any $B > 0, \epsilon > 0$,

$$\mathbb{P}\left(\sup_{\beta\in[0,B]} |\widehat{\tau}_{\beta K\epsilon} - t_\beta| \geq \epsilon\right) \leq C_1 e^{-C_2\epsilon^2\nu^{-1}}.$$

This establishes the theorem with $p = 1$. Of course, this system is Markov, so for $p > 1$ we simply bootstrap the same argument $p - 1$ times, and we are done.

□

References

[1] Alberts, B., Johnson, A., Lewis, J., Raff, M., Roberts, K., Walter, P. *Molecular Biology of the Cell.* Taylor and Francis, 4th edition, 2002.

[2] Astumian, R., Derenyi, I. Fluctuations driven transport and model of molecular motors and pumps. *European Biology Journal* **27** (1998), 474–489.

[3] Badoual, M., Julicher, F., Prost, J. Bidirectional cooperative motion of molecular motors. *Proceedings of the National Academy of Sciences of the United States of America*, **99**(10):6696–6701, 2002.

[4] DeVille, R., Muratov, C., Vanden-Eijnden, E. Two distinct mechanisms of coherence in randomly perturbed dynamical systems. *Phys. Rev. E (3)*, 72(3):031105, 10, 2005.

[5] DeVille, R., Muratov, C., Vanden-Eijnden, E. Non-meanfield deterministic limits in chemical reaction kinetics far from equilibrium. *Journal of Chemical Physics*, accepted May 2005.

[6] DeVille, R., Vanden-Eijnden, E. Self-induced stochastic resonance for brownian ratchets. *in preparation*, 2006.

[7] Duke, T. Molecular model of muscle contraction. *Proc. Nat. Acad. Sci. USA*, 96:2770–2775, March 1999.

[8] Elston, T., Peskin, C. The role of protein flexibility in molecular motor function: coupled diffusion in a titled periodic potential. *SIAM Journal of Applied Mathematics*, 60(3):842–867, 2000.

[9] Endow, S., Higuchi, H. A mutant of the motor protein kinesin that moves in both directions on microtubules. *Nature*, 406(6798):913–916, Aug 24 2000.

[10] Holmes, K. The swinging lever-arm hypothesis of muscle contraction. *Current Biology* 7 (2): R112-R118, Feb. 1 1997.

[11] Fisher, M., Kolomeisky, A. The force exerted by a molecular motor. *Proceedings of the National Academy of Sciences*, 96:6597–6601, June 1999.

[12] Fisher, M., Kolomeisky, A. Simple mechanochemistry describes the dynamics of kinesin molecules. *Proceedings of the National Academy of Sciences*, 98(14):7748–7753, 2001.

[13] Freidlin, M., Wentzell, A. *Random perturbations of dynamical systems.* Springer-Verlag, New York, second edition, 1998.

[14] Freidlin, M.. On stochastic perturbations of dynamical systems with fast and slow components. *Stoch. Dyn.*, 1(2):261–281, 2001.

[15] Freidlin, M.. On stable oscillations and equilibriums induced by small noise. *J. Statist. Phys.*, 103(1-2):283–300, 2001.

[16] Kolomeisky, A., Fisher, M. A simple kinetic model describes the processivity of myosin-V. *Biophysical Journal*, **84**:1642–1650, 2003.

[17] Muratov, C., Vanden-Eijnden, E., E, W. Self-induced stochastic resonance in excitable systems. *Phys. D*, **210**(3-4):227–240, 2005.

[18] Peskin, C., Oster, G. Coordinated hydrolysis explains the mechanical behavior of kinesin. *Biophysical Journal*, **68**:202–210, 1995.

[19] Rice, S., Lin, A. W., Safer, D., Hart, C. , Naber, N., Carragher, B., Cain, S., Pechatnikova, E., Wilson-Kubalek, E., Whittaker, M., Pate, E., Cooke, R., Taylor, E., Milligan, R., Vale, R. A structural change in the kinesin motor protein that drives motility. *Nature*, **402**(6763):778–784, DEC 16 1999.

[20] Rief, M., Rock, R., Mehta, A., Mooseker, M., Cheney, R., Spudich J. Myosin-V stepping kinetics: A molecular model for processivity. *Proc. Nat. Acad. Sci. USA*, **97**(17):9482–9486, 2000.

[21] Schilstra M., Martin, S. Viscous load imposes a regular gait on myosin-V. *Journal of the Royal Society – Interface*, **3**:153–165, 2006.

[22] Sellers, J. Myosins: a diverse superfamily. *Biochemica et Biophysica Acta*, **1496**(1):3–22, 2000.

[23] Shwartz, A., Weiss, A. *Large deviations for performance analysis.* Chapman & Hall, London, 1995.

[24] Vale, R., Milligan, R. The Way Things Move: Looking Under the Hood of Molecular Motor Proteins. *Science*, **288**: 88-95, 2000.